Equivalence of the virtual-source method and wave-field deconvolution in seismic interferometry

Roel Snieder,[1,*] Jon Sheiman,[2] and Rodney Calvert[2]
[1]*Center for Wave Phenomena and Department of Geophysics, Colorado School of Mines, Golden, Colorado 80401, USA*
[2]*Shell International Exploration and Production Inc., 3737 Bellaire Blvd., Houston, Texas 77001-0481, USA*
(Received 26 October 2006; published 23 June 2006)

Seismic interferometry and the virtual-source method are related approaches for extracting the Green's function that accounts for wave propagation between receivers by making suitable combinations of the waves recorded at these two receivers. These waves can either be excited by active, controlled, sources, or by natural incoherent sources. We compare this technique with the deconvolution of the wave field recorded at different receivers. We show that the deconvolved wave field is a solution of the same wave equation as that for the physical system, but that the deconvolved wave forms may satisfy different boundary conditions than those of the original system. We apply this deconvolution approach to the wave motion recorded at various levels in a building after an earthquake, and show how to extract the building response for different boundary conditions. Extracting the response of the system with different boundary conditions can be used to enhance, or suppress, the normal-mode response. In seismic exploration this principle can be used for the suppression of surface-related multiples.

DOI: 10.1103/PhysRevE.73.066620 PACS number(s): 46.40.−f, 45.30.+s, 43.40.+s

I. INTRODUCTION

Traditionally, imaging experiments rely on waves that are emitted by active sources that are recorded by an array of receivers. In seismic interferometry, also called *virtual source imaging*, one extracts the Green's function that accounts for the wave propagation between receivers by making suitable combinations of the waves recorded at these receivers. The recorded waves can be generated by a superposition of active sources, or might be excited by incoherent noise (e.g., Refs. [1–3]). This technique is useful because it obviates the need for an active, controlled source by replacing it by a receiver at the desired location.

Lobkis and Weaver [4] provide an elegant derivation of this principle based on normal-mode theory that is applicable to closed systems. It has been generalized to open systems [5–13]. The extraction of the Green's function has been applied to ultrasound data [14–16], helioseismology [17,18], surface waves in the Earth's crust [1–3,19], and the shallow subsurface [20], and seismic exploration [21–24]. In these applications the Green's function is extracted by correlation of observed wave forms. Snieder and Şafak [25] applied deconvolution of the motion recorded in a building to extract the building response from recordings of the incoherent motion of the building.

In this work we show that deconvolution of the motion recorded at several locations in a system can be used to retrieve the impulse response of that system. We also show that by deconvolving different combinations of the recorded waves, one can obtain the response of the system for different boundary conditions. This makes it possible to obtain the waves that would be recorded if the system were subject to boundary conditions that differ from those of the original physical system. Riley and Claerbout [26] coined the phrase *Noah's deconvolution* for this principle, and Wapenaar *et al.* [27] demonstrate this idea for a three-dimensional (3D) medium.

In Sec. II we show the motion recorded at various levels in the Robert A. Millikan Library in Pasadena, California, and show that deconvolution of the motion recorded at different levels gives the impulse response of the building. In Sec. III we show that the deconvolved waves satisfy the same wave equation as that of the original data, but that the boundary conditions of the deconvolved wave forms may differ from those of the system in which the data are recorded. In Sec. IV we apply this theory to the motion recorded in the Robert A. Millikan Library in Pasadena, California, and use it to extract the building response. We use these data to show in Sec. V that the deconvolved wave forms have a different resonance than does the physical building. In Sec. VI we show how the suppression of multiply reflected waves can be included in seismic interferometry.

II. DECONVOLUTION OF THE WAVES RECORDED IN THE MILLIKAN LIBRARY

We introduce the deconvolution of the wave forms with measurements of the acceleration measured in the basement and the ten floors of the Robert A. Millikan Library in Caltech after the Yorba Linda earthquake of 3 September 2002 (ML=4.8, time: 02:08:51 PDT, 33.917N 117.776W depth 3.9 km). The Millikan Library has been the focus of numerous studies on the building response and its temporal changes, e.g., Refs. [28–35]. The north-south component of the acceleration recorded in the west side of the building is shown in Fig. 1.

The motion in the building depends on the excitation of the building at the base, the coupling of the building to the subsurface, and the mechanical properties of the building. To unravel these different ingredients of the recorded motion, Snieder and Şafak [25] applied a deconvolution of the mo-

*Author to whom correspondence should be addressed. Email address: rsnieder@mines.edu

 ©2006 The American Physical Society

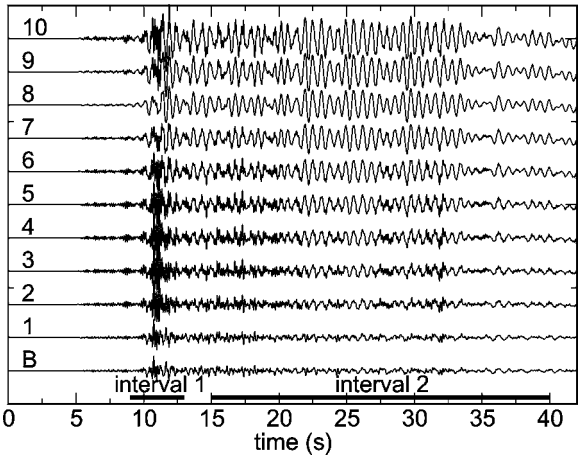

FIG. 1. The north-south component of the motion in the west side of the Millikan Library after the Yorba Linda earthquake of 3 September 2002 (ML=4.8, time: 02:08:51 PDT, 33.917N 117.776W depth 3.9 km). The floor numbers where the data are recorded are indicated at each trace. The bottom trace shows the wave recorded in the basement (B).

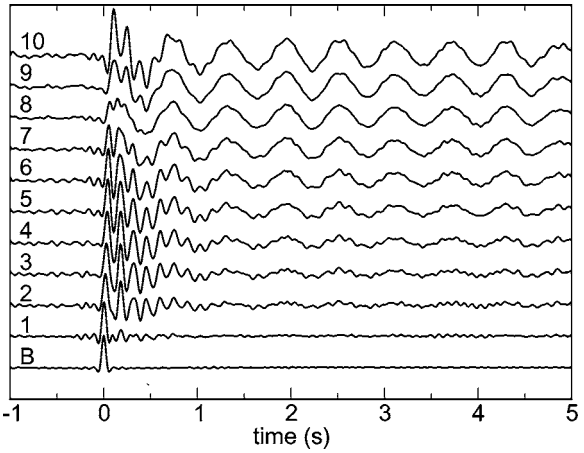

FIG. 2. The wave forms of Fig. 1 at the different floors after deconvolution with the waves recorded in the basement.

tion recorded at different levels in the building with the motion at a selected reference level. The deconvolution of the motion $u(\mathbf{r},\omega)$ recorded at location $\mathbf{r}$ with the motion recorded at location $\mathbf{r}_0$ is, in the frequency domain, given by

$$D(\mathbf{r},\mathbf{r}_0,\omega) = \frac{u(\mathbf{r},\omega)}{u(\mathbf{r}_0,\omega)}. \tag{1}$$

In the presence of noise, notches in the spectrum of $u(\mathbf{r}_0,\omega)$ cause numerical instabilities. For this reason we implemented the deconvolution numerically by using the conventional approach of "adding white noise:"

$$D(\mathbf{r},\mathbf{r}_0,\omega) = \frac{u(\mathbf{r},\omega)u^*(\mathbf{r}_0,\omega)}{|u(\mathbf{r}_0,\omega)|^2 + \varepsilon}. \tag{2}$$

In the examples that we show we set ε to 10% of the mean value of $|u(\mathbf{r}_0,\omega)|^2$, and we did not apply any filtering to the data. The regularized deconvolution (2) is not necessarily optimal. Various other approaches to deconvolution can be found in Ref. [36].

The waves deconvolved with the waves recorded in the basement are shown in Fig. 2. For the deconvolution in this example and all other examples, the wave forms shown in Fig. 1 between $t=0$ s and $t=40$ s have been used. The deconvolved wave in the basement is a bandpass-filtered delta function, because any signal deconvolved with itself, with white noise added, gives such a function. The deconvolved waves at the second floor and higher consist of a superposition of upgoing and downgoing waves for early times, while for later times the motion is dominated by a monochromatic resonance that decays exponentially with time. These deconvolved waves are analyzed in detail by Snieder and Şafak [25].

The deconvolved waves in Fig. 2 show a wave state of the building as if the motion at the base of the building were given by a delta function. For early times this pulse propagates upward in the building with a velocity given by the shear velocity of the building. At $t=0$, the wave field is nonzero only at the base of the building. This means that the wave field at that moment has collapsed onto a spatially localized pulse. This is reminiscent of the virtual source method [22,23], wherein waves recorded at different receivers are correlated to give a new wave field that corresponds to an impulsive source at one of the receivers. In this work we make the connection between the virtual source method and deconvolution, and illustrate this with the motion recorded in the Millikan Library.

III. PROPERTIES OF THE DECONVOLVED WAVE FIELD $D(\mathbf{r},\mathbf{r}_0,\omega)$

The connection between the deconvolved waves and the waves generated by a virtual source hinges on the *causality principle* which states that waves cannot move with a velocity higher than the maximum wave velocity c in the medium. Figure 3 illustrates this principle for the special case for one space dimension. The wave field at $z=z_0$ and time $t=0$ only influences the wave field in the grey-shaded region on the

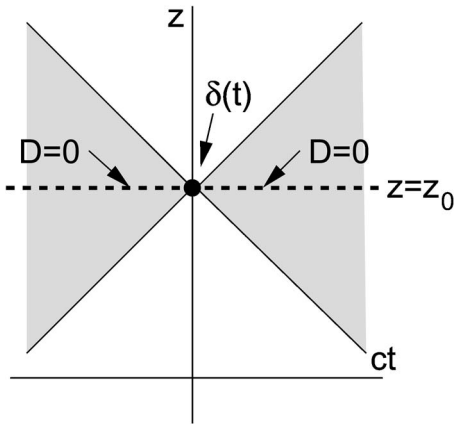

FIG. 3. The region where the solution is influenced by the wave field at $z=z_0$ and time $t=0$ (grey shading). $D(z,z_0,t)$ is nonzero only in this region. At $z=z_0$ this function is given by $D(z_0,z_0,t)=\delta(t)$.

right, and is influenced only be the wave field in the grey-shaded region on the left. By analogy with the jargon used in the theory of special relativity [37], we refer to these regions as the *light cones*. For a spatially variable velocity one could generalize the boundary of the light cones to be determined by the one-way travel time in the medium, but this refinement is not essential for the arguments used here. The second principle that we use, valid for a linear, time-invariant system, is given by the following theorem:

Theorem: In source-free regions $D(\mathbf{r},\mathbf{r}_0,\omega)$ satisfies the same wave equation as does $u(\mathbf{r},\omega)$.

To show this, let us suppose that the wave field satisfies

$$L(\mathbf{r},\omega)u(\mathbf{r},\omega)=0, \tag{3}$$

where L is a linear differential operator. [For example, for the Helmholtz equation $L=\nabla^2+\omega^2/c^2(\mathbf{r})$.] The right hand side of expression (3) is equal to zero because of the absence of sources. Applying the operator L to Eq. (1) gives

$$LD(\mathbf{r},\mathbf{r}_0,\omega)=L\frac{u(\mathbf{r},\omega)}{u(\mathbf{r}_0,\omega)}=\frac{1}{u(\mathbf{r}_0,\omega)}Lu(\mathbf{r},\omega)=0. \tag{4}$$

In the second identity we used that L acts on the $\mathbf{r}$ coordinate rather than on $\mathbf{r}_0$, and we used expression (3) in the last identity. Expression (4) proves that $D(\mathbf{r},\mathbf{r}_0,\omega)$ satisfies the same equation as does the wave field; therefore this quantity also satisfies the causality principle.

A number of comments can be made about this derivation. First, expression (4) holds in any number of dimensions. Second, the wave field $u(\mathbf{r},\omega)$ may be a vector field, and the operator L can be a matrix differential operator. The theorem still holds as long as the deconvolution is carried out with respect to linear superposition of the components of the wave field, or its derivatives. Third, suppose we had deconvolved two different solutions u_1 and u_2, both of which satisfy the differential equation (3) but with different boundary conditions. In that case the deconvolved wave form $D(\mathbf{r},\mathbf{r}_0,\omega)=u_1(\mathbf{r},\omega)/u_2(\mathbf{r}_0,\omega)$ also satisfies the differential equation (3). Fourth, we have shown that $D(\mathbf{r},\mathbf{r}_0,\omega)$ satisfies the same differential equation as does the wave field $u(\mathbf{r},\omega)$, but $D(\mathbf{r},\mathbf{r}_0,\omega)$ does not necessarily satisfy the same boundary conditions as does for $u(\mathbf{r},\omega)$. We show in Sec. V how this can be used to create virtual sources in a hypothetical system with boundary conditions that differ from those in the physical system. Fifth, the reasoning used for the deconvolved waves also applies to correlation of the waves, defined in the frequency domain by

$$C(\mathbf{r},\mathbf{r}_0,\omega)=u(\mathbf{r},\omega)u^*(\mathbf{r}_0,\omega). \tag{5}$$

$C(\mathbf{r},\mathbf{r}_0,\omega)$ satisfies the same wave equation as does $u(\mathbf{r},\omega)$; the proof is identical to that for the deconvolved waves. Finally, the wave field obtained by the regularized deconvolution (2) also satisfies the same wave equation as does the original system.

Definition (1) implies that $u(\mathbf{r},\omega)=D(\mathbf{r},\mathbf{r}_0,\omega)u(\mathbf{r}_0,\omega)$. In the time domain, this corresponds to

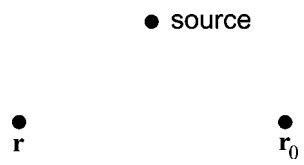

FIG. 4. Source-receiver geometry.

$$u(\mathbf{r},t)=\int D(\mathbf{r},\mathbf{r}_0,t')u(\mathbf{r}_0,t-t')dt'. \tag{6}$$

The function $D(\mathbf{r},\mathbf{r}_0,t')$ thus relates the wave field at $(\mathbf{r},t)$ to the wave field at $(\mathbf{r}_0,t-t')$. $D(\mathbf{r},\mathbf{r}_0,t')$ is a solution of the wave equation, but it is not necessarily equal to the Green's function that accounts for the wave propagation between $\mathbf{r}_0$ and $\mathbf{r}$. In the following we analyze the properties of the solution $D(\mathbf{r},\mathbf{r}_0,t')$ for the special case of one space dimension when no sources are present between the receivers, for which we can therefore use a causality principle.

The causality principle states that $u(\mathbf{r},t)$ and $u(\mathbf{r}_0,t')$ are unrelated when one of the space-time points lies outside of the light cone of the other space-time point. This principle holds for the physical wave field; for the deconvolved waves it means that

$$D(z,z_0,t)=0 \quad \text{for} \quad |t|<|z-z_0|/c. \tag{7}$$

This condition holds in one space dimension when there are no sources between z and z_0. To see the limitation of one space dimension consider the two-dimensional geometry of Fig. 4 wherein the distances from a source to two receivers are equal. For an isotropic source in a homogeneous medium, the waves recorded at the two receivers are identical; hence $D(\mathbf{r},\mathbf{r}_0,t)=\delta(t)$, which violates condition (7). In one dimension, when a source is present between receivers at locations z and z_0, the condition (7) does again not hold because the waves arriving at the two receivers will have a lag time smaller than $|z-z_0|/c$. In contrast when no sources are present between the receivers, the waves physically travel from one receiver to the other, and the causality condition (7) holds for the deconvolved waves.

Condition (7) implies that

$$D(z,z_0,t=0)=0 \quad \text{for} \quad z\neq z_0. \tag{8}$$

Furthermore, from definition (1)

$$D(z_0,z_0,\omega)=\frac{u(z_0,\omega)}{u(z_0,\omega)}=1, \tag{9}$$

so that in the time domain

$$D(z_0,z_0,t)=\delta(t). \tag{10}$$

These properties of the deconvolved waves are illustrated in Fig. 3. D is nonzero only in the gray-shaded light cone that corresponds to the point z_0 and time $t=0$. Along the line $z=z_0$, D is given by a delta function; hence

$$D(z_0,z_0,t)=0 \quad \text{for} \quad t\neq 0. \tag{11}$$

The wave field sketched in Fig. 3 corresponds for $t>0$ to the wave field excited by a point source at $z=z_0$ at time t

$=0$. Equation (4) states that this deconvolved wave field satisfies the same differential equation as the original wave field. As shown in Fig. 3, the wave field at $t=0$ is localized at the point z_0. For $t>0$ the waves radiate from that point and propagate into the medium. For $t>0$, the wave field is equal to the wave field that would be excited by a physical delta function source placed at z_0.

For $t<0$ the solution in Fig. 3 is nonzero as well. If a physical source would be present, the wave field could be quiescent for $t<0$. Because of the absence of a physical source, one calls the focused wave field at location z_0 at time $t=0$ a *virtual source*. The concept of virtual sources has been used in exploration seismology to create a wave field that emanates from a receiver in the subsurface [22,23]. For these reasons, the deconvolved waves are equivalent to a virtual source placed at $z=z_0$.

Note that because of condition (11), the deconvolved waves satisfy a boundary condition at $z=z_0$ that the original wave field, in general, does not satisfy. We can exploit this to create a wave field generated by a virtual source that satisfies more useful boundary conditions than does the original wave field.

The wave field sketched in Fig. 3 is identical to the wave field used by Rose [38]. At $t=0$ the wave field has collapsed onto a single point $z=z_0$. Rose shows that the solution of the Newton-Marchenko equation (an exact inverse-scattering method) corresponds to this special case. The difference between our approach and that of Rose [38] is that we assume that the wave field has been measured at z_0 whereas he shows how this wave field can be constructed from reflected and transmitted waves by solving the Newton-Marchenko equation.

The reader may wonder why we have deconvolved the wave field rather than applying another operation, such as correlation. Consider a multiplication with a general function $W(\omega)$ in the frequency domain that transforms the recorded waves $u(z,\omega)$ into a new wave field,

$$u_{new}(z,\omega) = W(\omega)u(z,\omega). \tag{12}$$

Let us ask the following question: what function $W(\omega)$ should we use so that the wave field at a target level z_0 is, in the time domain, given by a delta function? Since the delta function has a constant Fourier transform, this corresponds to the requirement

$$W(\omega)u(z_0,\omega) = 1. \tag{13}$$

Inserting the solution $W(\omega)=1/u(z_0,\omega)$ into expression (12) shows that the desired wave field is given by the deconvolution of $u(z,\omega)$ with $u(z_0,\omega)$. We show in Sec. VI how a different requirement can be used to compute a new wave field from the data that has upgoing waves only at a specified level.

IV. EXAMPLE, DECONVOLVED WAVE FORMS FOR THE MILLIKAN LIBRARY

As an example of the creation of a virtual source by deconvolution we show in Fig. 2 the wave forms at every level in the Millikan Library after a deconvolution with the waves recorded at the base of the building. This wave field is given by

$$D(z,z_{base},\omega) = \frac{u(z,\omega)}{u(z_{base},\omega)}, \tag{14}$$

where z_{base} denotes the location of the basement.

The deconvolved wave at the basement, the lower trace in Fig. 2, is given by a band-limited delta function. As shown in the previous section, this follows from the deconvolution collapsing the wave field at the target level into a delta function. Physically this operation corresponds to an interesting change in the wave field. The raw data in Fig. 1 recorded at the basement are a complex combination of an incoming P waves, incoming S waves, surface waves, and reflections of waves by the base of the building. The deconvolution collapses this complex wave field onto a band-limited delta function. Therefore the deconvolved wave field in Fig. 2 corresponds to the motion of the building as if it were excited by an impulsive excitation at the base, subject to the boundary condition that the base is otherwise fixed (Dirichlet boundary conditions).

Indeed, the deconvolved waves of Fig. 2 are excited by an upgoing traveling wave radiated by the delta function excitation at the base. This upward traveling wave reflects from the top of the building, and possibly also at intermediate levels, to create a downgoing wave. Between $t=0$ s and $t=1$ s, the deconvolved wave field consists primarily of a superposition of upward- and downward-going traveling waves. For later times, the deconvolved waves develop the character of a resonance of the building whose amplitude increases with the height in the building. This part of the signal corresponds to the normal modes of the building [25].

Note that the deconvolved waves in Fig. 2 are essentially zero before the first-arriving upward propagating wave. As shown in Sec. III, the deconvolved waves are nonzero only in the gray-shaded region shown in Fig. 3. (Since in Fig. 2 time, rather than ct, is shown along the horizontal axis, the first arriving waves appear at an angle that is much steeper than 45°.)

As a next example we show in Fig. 5 the wave field deconvolved with the waves recorded at the fifth floor. In the frequency domain, this deconvolved wave field is defined as

$$D(z,z_5,\omega) = \frac{u(z,\omega)}{u(z_5,\omega)}, \tag{15}$$

with z_5 the height of the fifth floor. Note that in Fig. 5 the trace at the fifth floor (marked in the left with the label "5") is a bandpass-filtered delta function. For positive time, an upward going and downward going wave are radiated from the fifth floor. The upward and downward going waves are followed by weaker waves caused by reflections within the building and from the base and the top of the building.

The deconvolved waves in Fig. 5 are acausal. For negative time, upward going and downward going waves are present that collapse onto a delta function at $t=0$ at the fifth floor. The deconvolved waves are acausal because there is no physical source at the fifth floor. Since the deconvolved

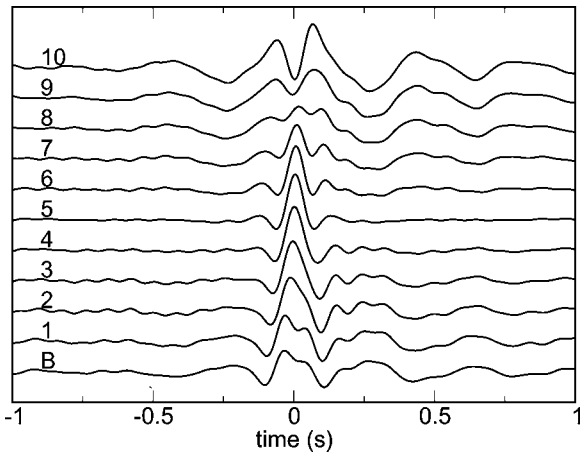

FIG. 5. The wave forms of Fig. 1 at the different floors after deconvolution with the waves recorded at the fifth floor.

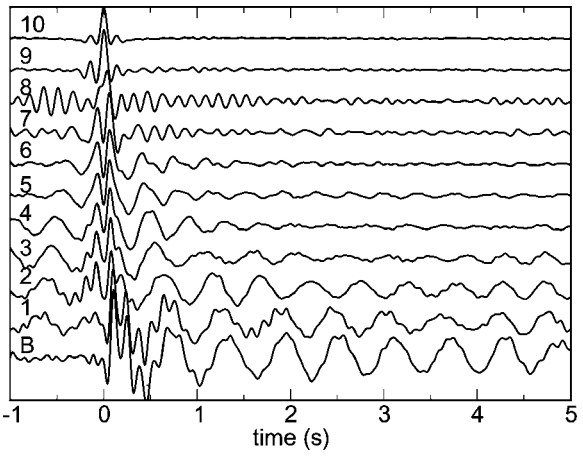

FIG. 6. The wave form recorded at the top floor deconvolved with the wave forms recorded at different floors.

waves satisfy the wave equation of the building, and since there is no physical source at the fifth floor, the deconvolved wave field must be nonzero at negative times in order to create a delta function response at the fifth floor; hence we speak of a virtual source. Note that the deconvolved waves in Fig. 5 show a bandpass-filtered version of the cartoon of Fig. 3 (again, with t rather than ct along the horizontal axis).

One may wonder why the wave forms obtained by deconvolution with the base of the building shown in Fig. 2 do not display acausal arrivals. The base of the building and the fifth floor are different because there is no physical source at the fifth floor, while the base of the building is being shaken by the earthquake. The shaking of the base of the building acts as an external source. Because of this external source, one does not need acausal arrivals to generate a wave field given by a delta function at the base of the building. The causality properties of the deconvolved wave field are thus related to the presence (or absence) of a physical source of the recorded waves.

V. CHANGED BOUNDARY CONDITION

In this section we describe a more subtle property of the wave field obtained by deconvolution with the motion at the base of the building, as shown in Fig. 2. In the building, downward propagating waves are reflected off the base of the building with a reflection coefficient $R(\omega)$. This reflection coefficient follows from the boundary conditions that the motion in the building satisfies. As shown in expression (10), and seen in the bottom trace of Fig. 2, the deconvolved wave field at the base of the building is given by a band limited delta function. The deconvolved wave field at the base of the building thus vanishes for $t \neq 0$. As argued in Sec. III, the deconvolved waves do not necessarily satisfy the same boundary conditions as those of the original wave field. The deconvolved wave field has a reflection coefficient

$$R_{dec} = -1 \tag{16}$$

at the base of the building. This can be seen as follows. According to expression (11) the deconvolved wave field at the base vanishes for $t \neq 0$. The only way in which this can happen is that a downgoing wave that strikes the base of the building is canceled by an upward traveling wave with the same strength and opposite polarity. This corresponds to the reflection coefficient $R_{dec}=-1$, which differs from the reflection coefficient $R(\omega)$ of the building.

A change in the boundary conditions at the base of the building should change the corresponding normal modes. A building of height H and shear velocity c, and a reflection coefficient -1 at its base, has a fundamental mode period that is given by [39]

$$T = \frac{4H}{c}. \tag{17}$$

The deconvolved waves have a reflection coefficient -1 at the target level z_0. This means that the wave field obtained by deconvolution of the wave field above the target level z_0 is equal to the wave field of a fictitious building that is cut off at height z_0 and that has reflection coefficient -1 at that level. Following expression (17), the fundamental mode of that fictitious building has a period

$$T_{new} = \frac{4(H - z_0)}{c}. \tag{18}$$

In order to illustrate this, we show in Fig. 6 the wave field at the top floor deconvolved with the wave field at different target levels; i.e., this figure shows

$$f(z, \omega) = \frac{u(H, \omega)}{u(z, \omega)}. \tag{19}$$

This deconvolved wave field differs from that shown in Fig. 2 because that figure shows that wave field at every level deconvolved with the waves recorded at a fixed level (the base), while Fig. 6 shows the wave field at one level (the top) deconvolved with waves recorded at different levels. Setting $z=H$ in expression (19) gives unity in the right hand side. In the time domain this corresponds to the band-limited delta function in the top trace of Fig. 6.

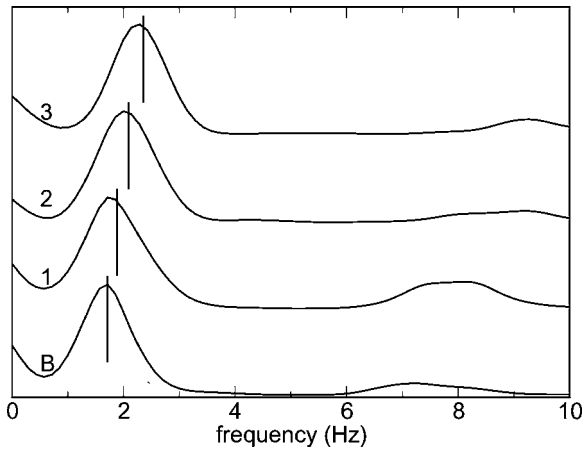

FIG. 7. Amplitude spectra of the deconvolved waves of Fig. 6 for the basement and lower three floors of the building. The vertical lines give an estimate of the normal mode of the building that is truncated at the corresponding height.

The lowest three traces of Fig. 6 show a damped normal mode whose period decreases with increasing floor number. This can be seen in the amplitude spectrum of the deconvolved motion at the lowest four levels, shown in Fig. 7. Indicated by the vertical lines in that figure are the normal-mode frequencies of expression (18). The normal-mode frequencies of this fictitious building explain the resonance of the deconvolved wave field well. This is an experimental confirmation that the deconvolved wave field indeed satisfies boundary conditions that differ from those of the original wave field.

VI. MULTIPLE REMOVAL BY DECONVOLUTION WITH UPGOING WAVES

Imaging techniques used in radar imaging and reflection seismology are based on singly reflected waves. In reflection seismology these waves are referred to as *primaries*. In practice one does not record only the singly reflected waves because multiply reflected waves are also present in the data. In exploration seismology, these multiply reflected waves are referred to as *multiples*. The strongest multiples are those reflected from the Earth's free surface; these are called *surface-related multiples* (e.g., Refs. [40–43]). In marine seismic surveys the multiples reflected at the sea surface are strong because they have a reflection coefficient for pressure of approximately -1.

In reflection seismology one often seeks to remove the surface-related multiples because they may be erroneously imaged onto spurious reflectors that are not present in the subsurface. In the absence of a free surface, the only downgoing wave at receivers placed above reflectors would be due to the wave excited by the source. Then, one would record the one downgoing wave excited by the source, plus upgoing waves that are generated by reflectors in the Earth. (These reflected waves consist of singly reflected waves and internal multiples that are multiple reflections between layers in the subsurface.) Now suppose that the free surface is present, then the downgoing waves recorded at the receivers consist

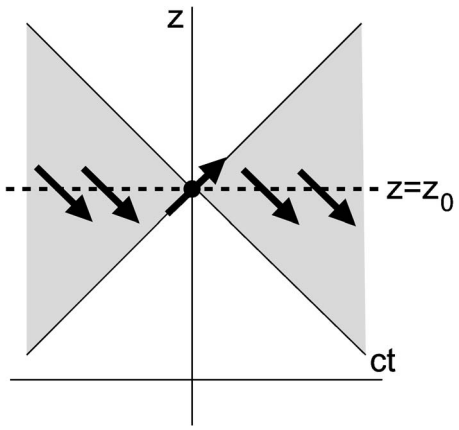

FIG. 8. The region where $D(z,z_0,t)$ is nonzero, (shown by grey shading). At $z=z_0$ this function has downgoing waves only, except at $t=0$ where a delta function pulse is moving upwards.

of the direct wave that is excited by the source, plus all the waves that are reflected from the free surface. This suggests that if we want to remove the surface-related multiples, we need to manipulate the data in such a way that the downgoing wave field consists of the direct downgoing wave only. We have seen in the previous section that we can change the boundary conditions of the wave field by carrying out a suitable deconvolution of the wave field recorded at different levels.

In the example of exploration seismology, the source and the free surface are above the region of interest. For the Millikan Library the earthquake excites the building from below, and the building extends upward. For this reason, the roles of "up" and "down" are reversed in exploration seismology and in the Millikan Library. In the following we focus on the Millikan Library. It is our goal to manipulate the data in such a way that reflections from the base of the building correspond to surface-related multiples that we wish to remove.

In the following we use that the wave field can be decomposed in upgoing waves u_+ and downgoing waves u_-:

$$u(z,\omega) = u_+(z,\omega) + u_-(z,\omega). \tag{20}$$

The multiple reflections at the base of the building are removed by deconvolving the wave field at every level with the upgoing wave at the base of the building to give

$$D_+(z,z_0,\omega) = \frac{u(z,\omega)}{u_+(z_0,\omega)}. \tag{21}$$

By inserting the decomposition (20) into this expression one obtains for the target level $z=z_0$:

$$D_+(z_0,z_0,\omega) = 1 + \frac{u_-(z_0,\omega)}{u_+(z_0,\omega)}. \tag{22}$$

The first term corresponds, in the time domain, to a delta function, while the second term contains downgoing waves in the numerator. Note that it is immaterial whether z_0 is the base of the building or an arbitrary level.

The wave state (21) is sketched in Fig. 8. Since $D(z,z_0,\omega)$

satisfies the wave equation of the building, this function has the same causality properties as the original wave field, and the solution is nonzero in the grey-shaded region only. According to expression (22) the upgoing wave at the target level z_0 is given by a delta function. Apart from this impulsive upgoing wave, there are only downgoing waves at that level. The last term of expression (22) gives the reflection response that is, in the frequency domain, defined as the ratio of the waves propagating in the "+" and "−" directions:

$$r(\omega) = \frac{u_-(z_0,\omega)}{u_+(z_0,\omega)}. \tag{23}$$

The wave field (21) thus constitutes the motion of the building for an impulsive wave launched upward on the building at the target level z_0, and for which only downward-going waves are present at that level for $t \neq 0$. When the target level is the base of the building this procedure removes the surface-related multiples, because all reflections from the base of the building are compressed by the deconvolution into a single upgoing delta function. Since for $t \neq 0$ only downgoing waves exist at the base of the building, this wave state satisfies radiation boundary conditions at the target level z_0 (Fig. 8).

In our example of the Millikan Library the dominant wavelength is much larger than the width of the building, and the wave propagation is quasi-one-dimensional. In that case the separation of upgoing and downgoing waves can be achieved by using that, in the time domain, the upgoing and downgoing waves satisfy [44]

$$\frac{\partial u_+}{\partial t} = \frac{1}{2}\left(\frac{\partial u}{\partial t} - c\frac{\partial u}{\partial z}\right),$$

$$\frac{\partial u_-}{\partial t} = \frac{1}{2}\left(\frac{\partial u}{\partial t} + c\frac{\partial u}{\partial z}\right). \tag{24}$$

We computed $\partial u/\partial z$ by computing the finite difference of the waves recorded at the target level z_0 and the adjacent level above using the wave velocity $c = 322$ m/s obtained by Snieder and Şafak [25] from a normal-mode analysis of the Millikan Library.

Figure 9 shows the wave field (21) after deconvolving the motion at every level with the upgoing wave in the basement. An upward-propagating wave is launched from the base of the building that is reflected by the top of the building, and, to a lesser extent, by the floors within the building. A comparison with Fig. 2 is interesting. (Note that the figures have a different time scale.) Figure 2, obtained by deconvolution with the full wave field at the base, displays a strong resonance that is absent in Fig. 9. The physical reason for this is that, as shown in Sec. IV, the deconvolved waves of Fig. 2 give the motion of the building when the reflection coefficient at the base is equal to −1. This strong reflection coefficient causes the pronounced normal mode in Fig. 2. By contrast, the wave field in Fig. 9 has, apart from an impulsive upgoing waves, only downgoing waves at the base of the building. This solution therefore satisfies a radiation boundary condition at the base that precludes normal-mode solutions. This is another example that the deconvolved wave field may satisfy other boundary conditions than those of the original wave field.

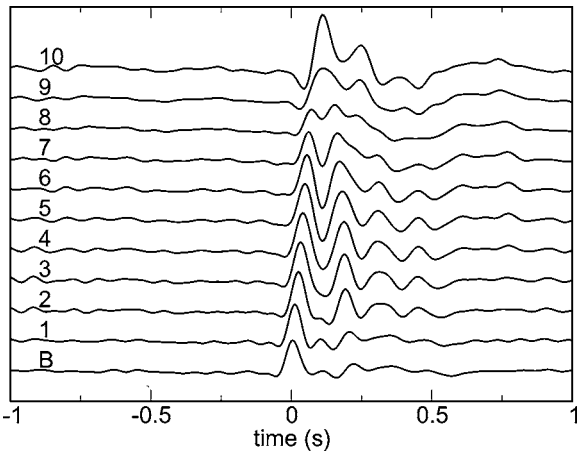

FIG. 9. The wave forms of Fig. 1 at every floor deconvolved with the upgoing wave in the basement.

One can, of course, also carry out a deconvolution with respect to the downgoing waves at the target level, defined as

$$D_-(z,z_0,\omega) = \frac{u(z,\omega)}{u_-(z_0,\omega)}. \tag{25}$$

Using the basement as the target level this deconvolved wave field is shown in Fig. 10. This figure should be compared with Fig. 9, obtained for deconvolution with respect to the upgoing wave. The deconvolved waves in Fig. 10 have an impulsive downgoing wave at the base; apart from this wave the waves propagate upward at that level. This solution is acausal. Physically it corresponds to a solution where acausal upward propagating waves are launched at the base of the building so that only one downward going impulsive wave at $t=0$ is present at the base of the building. Note that Fig. 10 is not the time-reversed version of Fig. 9, as one might perhaps expect. The Millikan Library displays a significant intrinsic attenuation [25], which breaks the invariance for time reversal [45,46].

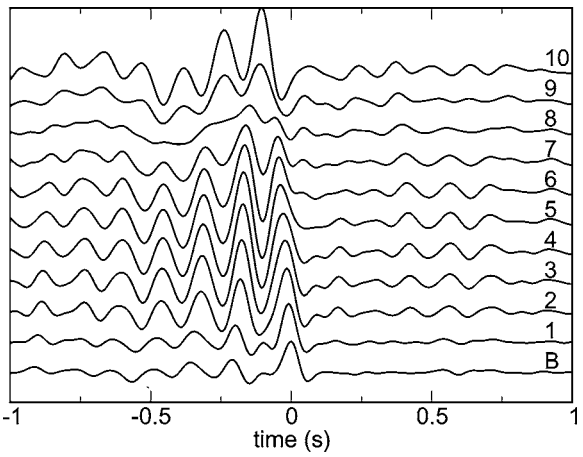

FIG. 10. The wave forms of Fig. 1 at every floor deconvolved with the downgoing wave in the basement.

Figure 9 gives the motion of the building when an upward propagating impulsive wave is launched at the base of the building, and where the reflected waves satisfy a radiation boundary condition at the base. The attenuation in the building causes a decay of the waves with time. By contrast, the solution of Fig. 10 gives the motion of the building where upward propagating waves at the base of the building cause a downward propagating impulsive wave at the base at $t=0$. Because of the attenuation in the building, these upward propagating waves, and their reflection, also decay with increasing time. To correct for this attenuation, the upward propagating waves are stronger than they would be in the absence of intrinsic attenuation. These effects combined cause the waves in Fig. 10 to be stronger than those in Fig. 9.

In the Millikan Library, the wave propagation is essentially in one dimension for the employed frequencies. The generalization of the ideas presented here to exploration geophysics involves the nontrivial extension to more space dimensions. A possible way to achieve this is to make a plane-wave decomposition of the data. When the three components of the data are known at the free surface, or the pressure and the three components of the displacement are known at the ocean floor, one can separate the wave field in upgoing and downgoing waves [44,47].

VII. DISCUSSION

We have shown that the deconvolution of the waves recorded at different locations leads to a new solution of the system that governs the waves, but in general with different boundary conditions. The associated change in the boundary conditions can be useful for practical purposes.

In Sec. V we used this property to obtain the motion of the Millikan Library as if its base had been fixed. In general, the attenuation of waves in buildings depends on both the intrinsic attenuation and the radiation damping at the base of the building. The deconvolved waves have a reflection coefficient -1 rather than the physical reflection coefficient $R(\omega)$. The radiation damping that is associated with a reflection coefficient $|R(\omega)|<1$ has been eliminated from the problem by considering the waves deconvolved with the motion of the base. This makes it possible to separate the contributions of anelastic attenuation and radiation damping.

By carrying out the deconvolution with respect to the upgoing waves at one level, we create yet another state in the building, one for which the boundary condition is a radiation boundary condition. In this wave state, reflections from the base of the building have been switched off. This principle can also be used in seismic exploration for the suppression of surface-related multiples. The similarity of the deconvolution approach presented here and the virtual-source method [22,23] suggests that it is possible to reformulate the virtual-source method to include changes in the boundary conditions as well. This may make it possible to fold the elimination of surface-related multiples into the virtual-source method.

ACKNOWLEDGMENTS

We thank Ken Larner, Paul Martin, and Paul Sava for their critical and constructive comments. This research was supported by the Gamechanger Program of Shell International Exploration and Production Inc.

[1] N. M. Shapiro and M. Campillo, Geophys. Res. Lett. **31**, L07614 (2004).
[2] N. M. Shapiro, M. Campillo, L. Stehly, and M. H. Ritzwoller, Science **307**, 1615 (2005).
[3] K. G. Sabra, P. Gerstoft, P. Roux, W. A. Kuperman, and M. C. Fehler, Geophys. Res. Lett. **32**, L03310 (2005).
[4] O. I. Lobkis and R. L. Weaver, J. Acoust. Soc. Am. **110**, 3011 (2001).
[5] A. Derode, E. Larose, M. Tanter, J. de Rosny, A. Tourin, M. Campillo, and M. Fink, J. Acoust. Soc. Am. **113**, 2973 (2003).
[6] A. Derode, E. Larose, M. Campillo, and M. Fink, Appl. Phys. Lett. **83**, 3054 (2003).
[7] P. Roux, K. G. Sabra, W. A. Kuperman, and A. Roux, J. Acoust. Soc. Am. **117**, 79 (2005).
[8] R. Snieder, Phys. Rev. E **69**, 046610 (2004).
[9] R. Snieder, K. Wapenaar, and K. Larner, Geophysics (to be published).
[10] K. Wapenaar, Phys. Rev. Lett. **93**, 254301 (2004).
[11] K. Wapenaar, J. Fokkema, and R. Snieder, J. Acoust. Soc. Am. **118**, 2783 (2005).
[12] R. L. Weaver and O. I. Lobkis, J. Acoust. Soc. Am. **116**, 2731 (2004).
[13] R. L. Weaver and O. I. Lobkis, J. Acoust. Soc. Am. **117**, 3432 (2005).
[14] R. L. Weaver and O. I. Lobkis, Phys. Rev. Lett. **87**, 134301 (2001).
[15] R. Weaver and O. Lobkis, Ultrasonics **40**, 435 (2003).
[16] A. E. Malcolm, J. A. Scales, and B. A. van Tiggelen, Phys. Rev. E **70**, 015601(R) (2004).
[17] J. E. Rickett and J. F. Claerbout, in *Helioseismic Diagnostics of Solar Convection and Activity*, edited by T. L. Duvall, J. W. Harvey, A. G. Kosovichev, and Z. Svestka (Kluwer Academic Publishers, Dordrecht, 2001).
[18] J. E. Rickett and J. F. Claerbout, The Leading Edge **18**, 957 (1999).
[19] M. Campillo and A. Paul, Science **299**, 547 (2003).
[20] J. N. Louie, Bull. Seismol. Soc. Am. **91**, 347 (2001).
[21] J. F. Claerbout, Geophysics **33**, 264 (1968).
[22] R. W. Calvert, A. Bakulin, and T. C. Joners, Expanded abstracts of the 2004 EAEG-meeting, 2004.
[23] A. Bakulin and R. Calvert, Expanded abstracts of the 2004 SEG-meeting, 2004, pp. 2477–2480.
[24] G. T. Schuster, J. Yu, J. Sheng, and J. Rickett, Geophys. J. Int. **157**, 838 (2004).
[25] R. Snieder and E. Şafak, Bull. Seismol. Soc. Am. **96**, 586 (2006).
[26] D. C. Riley and J. F. Claerbout, Geophysics **41**, 592 (1976).
[27] K. Wapenaar, J. Thorbecke, and D. Dragonov, Geophys. J. Int.

156, 179 (2004).
[28] P. C. Jennings and J. H. Kuroiwa, Bull. Seismol. Soc. Am. **58**, 891 (1968).
[29] F. E. Udwadia and M. D. Trifunac, Earthquake Eng. Struct. Dyn. **2**, 359 (1974).
[30] D. A. Foutch, J. E. Luco, M. D. Trifunac, and M. E. Udwadia, in *Proceedings, U.S. National Conference on Earthquake Engineering*, 1975, pp. 206–215.
[31] F. E. Udwadia and P. Z. Marmarelis, Bull. Seismol. Soc. Am. **66**, 121 (1976).
[32] D. A. Foutch and P. C. Jennings, Bull. Seismol. Soc. Am. **68**, 219 (1978).
[33] J. Luco, M. Trifunac, and H. Wong, Bull. Seismol. Soc. Am. **77**, 1961 (1987).
[34] J. F. Clinton, Ph.D. thesis, California Institute of Technology, 2004.
[35] S. C. Bradford, J. F. Clinton, and T. H. Heaton, in *Proceedings of the Structures Congress and Exposition, Metropolis and Beyond - Proceedings of the 2005 Structures Congress and the 2005 Forensic Engineering Symposium*, 2005, pp. 887–897.
[36] *Deconvolution*, edited by G. M. Webster, Geophysics reprint series, Vol. 1 (SEG, Tulsa, 1978).
[37] H. Ohanian and R. Ruffini, *Gravitation and Spacetime*, 2nd edition (Norton & Co., New York, 1994).
[38] J. H. Rose, in *Imaging of Complex Media with Acoustic and Seismic Waves*, edited by M. Fink, W. A. Kuperman, J. P. Montagner, and A. Tourin (Springer, Berlin, 2002), pp. 97–106.
[39] A. K. Chopra, *Dynamics of Structures; Theory and Applications to Earthquake Engineering*, second edition (Prentice-Hall, Englewood Cliffs, NJ, 1995).
[40] W. H. Dragoset and Z. Jeričević, Geophysics **63**, 772 (1998).
[41] B. L. N. Kennett, Geophys. Prospect. **27**, 584 (1979).
[42] R. G. van Borselen, J. T. Fokkema, and P. M. van den Berg, Geophysics **61**, 202 (1996).
[43] D. J. Verschuur, A. J. Berkhout, and C. P. A. Wapenaar, Geophysics **57**, 1166 (1992).
[44] E. A. Robinson, in *Handbook of Geophysical Exploration*, edited by K. Helbig and S. Treitel (Pergamon, Amsterdam, 1999), Vol. 4B.
[45] M. Fink, Phys. Today **50**, 34 (1997).
[46] R. Snieder, in *Imaging of Complex Media with Acoustic and Seismic Waves*, edited by M. Fink, W. A. Kuperman, J. P. Montagner, and A. Tourin (Springer, Berlin, 2002), pp. 1–15.
[47] C. P. A. Wapenaar, P. Herrmann, D. J. Verschuur, and A. J. Berkhout, Geophys. Prospect. **38**, 633 (1990).